Synthesis of the superheavy elements beyond Og: extrapolating from ^{48}Ca to ^{50}Ti and ^{54}Cr*

Yueping Fang (方岳平)[1] Long Zhu (祝龙)[1,2†]

[1]Sino-French Institute of Nuclear Engineering and Technology, Sun Yat-sen University, Zhuhai 519082, China
[2]Guangxi Key Laboratory of Nuclear Physics and Nuclear Technology, Guangxi Normal University, Guilin 541004, China

Abstract: Theoretical predictions on the optimal reaction energies are essential for producing superheavy elements (SHEs) beyond Og. Due to the limitation of the targets, synthesizing elements 119 and 120 will require beams of ^{50}Ti and/or ^{54}Cr ions. However, is it reliable to theoretically extrapolate from the well-investigated ^{48}Ca induced reactions to those with heavier projectiles? In this work, we answer this question from two perspectives: radial and mass asymmetry degrees of freedom. The Smoluchowski diffusion equation is employed in the mass asymmetry degree of freedom for the first time, in which by fitting the calculations to experimental evaporation residue cross sections (ERCS) for the reactions of ^{48}Ca as projectiles with the actinide targets, a strong linear correlation between the contact distance ($D_{\rm cont}$) and center-of-mass energy excess above the Coulomb barrier ($E_{\rm c.m.}-B_0$) is found and a parametrization formula is introduced. The calculations based on the fitted formula satisfactorily reproduce the available experimental data of the ERCS. Furthermore, thanks to the recent experimental data, we extrapolate the calculation in the reactions ^{50}Ti + ^{242}Pu, ^{50}Ti + ^{244}Pu, and ^{54}Cr + ^{238}U. The calculations reproduce the experimental data rather well within the experimental errors in both perspectives. Our results demonstrate that theoretically extrapolating the projectile from ^{48}Ca to ^{50}Ti and ^{54}Cr for synthesizing SHEs beyond Og is relatively reliable.

Keywords: Superheavy nuclei, Fusion reaction, Smoluchowski diffusion equation, Evaporation residue cross section

DOI: **CSTR:**

I. INTRODUCTION

The synthesis of superheavy elements (SHEs) is a frontier of research in nuclear physics [1−5]. With regard to the hot fusion reactions, a remarkable progress has been made in the synthesis of SHEs by employing double magic projectile ^{48}Ca and actinide targets [6−10]. In recent years, to open the eighth period, worldwide efforts have been made to produce SHEs beyond Oganesson (Og). Unfortunately, no correlated decay chains were observed. A key challenge is determining the optimal incident energy (OIE), which mainly depends on theoretical predictions [5, 11, 12].

It is worth noting that because of the plenty of experimental data, most of the theories can describe the ^{48}Ca induced fusion-evaporation reactions quite well. However, in order to synthesize SHEs beyond Og, projectiles heavier than ^{48}Ca such as ^{50}Ti, ^{54}Cr, ^{58}Fe, and ^{64}Ni are considered among the most promising candidates [13]. Is it reliable to extrapolate theoretically from the well-investigated ^{48}Ca induced reactions to those with heavier projectiles for predicting the OIEs?

Due to the complexity of the synthesis mechanisms of SHEs, particularly the presence of delicate ambiguities [14], the fusion process is not well understood theoretically[15, 16]. The fusion probability is particularly important for revealing the mechanism of synthesizing the SHEs, which is usually calculated by using diffusion models [17, 18], master equations [19−29], or empirical formulas [30]. These theories describe the dynamics of the formation of compound nuclei from different degrees of freedom, mainly at the radial degree of freedom: distance $\vec{R}$ between the centers of the nuclei (corresponding to the elongation of a mononucleus) and the mass asymmetry degree of freedom: $\eta=\frac{A_1-A_2}{A_1+A_2}$ (A_1 and A_2 are the mass numbers of the two nuclei that make up the compound nuclei).

Owing to these inherent ambiguities and the diversity

Received 31 January 2026; Accepted 10 June 2026

* This work was supported by the National Natural Science Foundation of China under Grants No. 12075327 and 12475136; The Open Project of Guangxi Key Laboratory of Nuclear Physics and Nuclear Technology under Grant No. NLK2022-01; Fundamental Research Funds for the Central Universities, Sun Yat-sen University under Grant No. 23lgbj003

† E-mail: zhulong@mail.sysu.edu.cn

of theoretical frameworks, the reliability of predictions for SHEs with Z=119 and 120 has become an urgent concern. Currently, most theoretical models describe existing experiments fairly well. However, despite extensive theoretical studies on the synthesis of SHEs with Z=119 and 120, predictions across different theoretical models exhibit significant uncertainty and model dependence[5]. In this case, it is imperative to address several critical aspects to provide reliable theoretical predictions: (i) How to evaluate the uncertainty of the theoretical model? In Ref. [31], the Bayesian uncertainty quantification method is employed to evaluate the uncertainty of the calculated ERCS in the dinuclear system model. (ii) How can we reduce the model dependence of theoretical predictions? One weak model-dependence method (the OIE law) is proposed based on the strong correlation between the OIEs, the Coulomb barrier height of side collision, and the Q value [11]. (iii) Is it reliable to extrapolate predictions from ^{48}Ca to ^{54}Cr? In this work, utilizing the latest experimental data of ^{50}Ti and ^{54}Cr projectiles introduced reactions [5, 13], we quantify the reliability of extrapolation from ^{48}Ca to ^{54}Cr within a one-dimensional model by employing the Smoluchowski diffusion equation, which is examined from two distinct perspectives: the radial degree of freedom and the mass asymmetry degree of freedom.

The Smoluchowski diffusion equation provides a concise physical image, in which the fusion probability is described by an analytical formula. It has been effectively applied in the investigation of the SHEs synthesis based on the radial degree of freedom for both cold and hot fusion reactions [17, 32−34]. During the fusion stage, the system undergoes diffusion across a one-dimensional parabolic barrier to overcome the fusion barrier and form the compound nucleus. Also, as shown in the following, the only adjustable parameter is obtained from systematic behaviors, which will relatively reduce the uncertainty introduced by the theoretical model, making it well suited to investigate the extrapolation properties. In the present study, we adopt the Smoluchowski diffusion equation to investigate the theoretical extrapolation ability from ^{48}Ca to heavier projectiles (^{50}Ti/^{54}Cr) for synthesizing the SHEs. In order to strengthen the reliability, in addition to the radial degree of freedom we also employ the Smoluchowski diffusion equation in the mass asymmetry degree of freedom for the first time.

II. THEORETICAL DESCRIPTIONS

Theoretically, the synthesis of SHEs can be divided into three steps and the ERCS is calculated as the summation over all partial waves J:

$$\sigma_{\rm ER}(E_{\rm c.m.}) = \frac{\pi\hbar^2}{2\mu E_{\rm c.m.}}\sum_J (2J+1)T(E_{\rm c.m.},J)P_{\rm fus}(E_{\rm c.m.},J)W_{\rm sur}(E^*,J), \quad (1)$$

where $E_{\rm c.m.}$ denotes the incident energy in the center-of-mass system. The excitation energy $E^* = E_{\rm c.m.} + {\rm Q}$. The values of Q calculated by using the Myers mass table [35]. $T(E_{\rm c.m.},J)$ is the transmission probability. $P_{\rm fus}(E_{\rm c.m.},J)$ is the fusion probability and $W_{\rm sur}(E_{\rm c.m.},J)$ denotes the survival probability.

In the capture process, the projectile nucleus overcomes the Coulomb potential barrier to form a dinuclear system. The calculation of the Coulomb barrier relies on the nucleus-nucleus interaction potential. The interaction potential consists of Coulomb potential $V_{\rm C}$ and nuclear potential $V_{\rm N}$. $V_{\rm C}$ is written by Wong formula:

$$\begin{aligned} &V_C(R,\beta_1,\beta_2,\theta_1,\theta_2) \\ &= \frac{Z_1Z_2e^2}{R} + \sqrt{\frac{9}{20\pi}}\left(\frac{Z_1Z_2e^2}{R^3}\right)\sum_{i=1,2}R_i^2\beta_2^{(i)}P_2(\cos\theta_i) \\ &+ \left(\frac{3}{7\pi}\right)\left(\frac{Z_1Z_2e^2}{R^3}\right)\sum_{i=1,2}R_i^2\left[\beta_2^{(i)}P_2(\cos\theta_i)\right]^2. \end{aligned} \quad (2)$$

$V_{\rm N}$ is written by the double-folding method:

$$\begin{aligned} V_{\rm N}(\mathbf{R}) = C_0\Big\{&\frac{F_{\rm in}-F_{\rm ex}}{\rho_0}\Big[\int\rho_1^2(\mathbf{r})\rho_2(\mathbf{r}-\mathbf{R})d\mathbf{r} \\ &+\int\rho_1(\mathbf{r})\rho_2^2(\mathbf{r}-\mathbf{R})d\mathbf{r}\Big] \\ &+F_{\rm ex}\int\rho_1(\mathbf{r})\rho_2(\mathbf{r}-\mathbf{R})d\mathbf{r}\Big\}, \end{aligned} \quad (3)$$

ρ_1 and ρ_2 are the nuclear density distribution functions. Details can be found in Ref. [31].

Since the OIE for the SHEs synthesis reactions investigated in this work is dominated by the 3n evaporation channel at high excitation energies, the influence of barrier distributions is weak for determining OIE. Therefore, to avoid introducing empirical parameters and to minimize model uncertainty, we only consider simple single-barrier penetration without empirical barrier distribution in the capture process. The penetration probability is given by the well-known Hill-Wheeler formula [36]:

$$T(E_{\rm c.m.},J) = \frac{1}{1+\exp\left\{-\frac{2\pi}{\hbar\omega(J)}\left[E_{\rm c.m.}-B-\frac{\hbar^2}{2\mu R_{\rm B}^2(J)}J(J+1)\right]\right\}}, \quad (4)$$

the interaction potential at the maximum is defined as the

barrier height B, and the corresponding position is the barrier radius $R_{\rm B}(J)$ for the Jth partial wave. Taking the interaction potential of reaction ^{48}Ca + ^{243}Am as an example, we demonstrate the B and $R_{\rm B}$ in Fig. 1. The potential around the Coulomb barrier can be approximated by an inverted parabola with curvature $\hbar\omega(J)$. The barrier curvature $\hbar\omega(J)$ can be calculated using the formula $\hbar\omega(J) = \sqrt{-\frac{\hbar^2}{\mu}\frac{\partial^2}{\partial R^2}V(R,J)}\Big|_{R=R_{\rm B}(J)}$.

$P_{\rm fus}$ is calculated by using the Smoluchowski diffusion equation [37]:

$$G\frac{\partial W}{\partial {\rm t}} = -(bxW)' + TW''. \tag{5}$$

The Brownian particle moves along the stretching degree of freedom x in a viscous fluid, which is characterized by a repulsive parabolic potential $V(x) = -bx^2/2$. The constant G is a friction coefficient. The initial probability distribution W is assumed to be a delta function at the event injection point $S_{\rm inj}$. And it is assumed that W is a Gaussian distribution function that elongates over time. When the interaction time approaches infinity, the probability of the Gaussian distribution being on the right side of the maximum point of the potential barrier is:

$$P_{\rm fus}(E_{\rm c.m.},J) = \frac{1}{2}(1 - {\rm erf}\sqrt{\frac{B_{\rm fus}(J)}{T}}). \tag{6}$$

The $P_{\rm fus}(E_{\rm c.m.},J)$ results from the angular momentum (J)-dependent potential energy surface of the colliding system. T is the temperature of the fusing system. $B_{\rm fus}(J)$ is the inner fusion barrier that a binuclear system must overcome to form a compound nucleus during the subsequent fusion process after capture. We study the complex fusion process in terms of the evolution of two degrees of freedom, radial and mass asymmetry degrees of freedom, respectively. In this study, we neglected shell effects during the fusion process. For hot fusion reactions with relatively high excitation energy, these effects are largely suppressed, making this approximation reasonable[73]. In particular, when the excitation energy reaches 30–50 MeV, the temperature dependent shell effects may have a minimal impact on the fusion barrier. Furthermore, as described by W.J. Swiatecki[17], the smooth parabolic parameterization of the potential energy surface adopted in this work facilitates the derivation of analytical expressions in Eq. (3). Finally, this systematic analysis of parameters effectively reduces the errors introduced by neglecting shell effects, ensuring that our calculated results remain relatively reliable. Specific details are discussed in later.

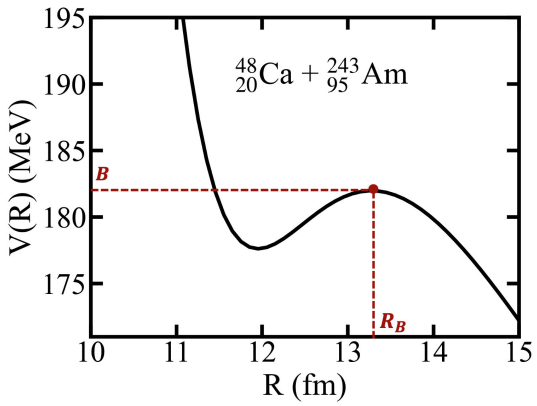

Fig. 1. (Color online) Nucleus-nucleus interaction potential of reaction ^{48}Ca + ^{243}Am.

The excited compound nucleus can evaporate light particles, such as neutrons, protons, and α particles. We employ the Monte Carlo method to calculate the decay probabilities in each channel. In the ith deexcitation step the probability of evaporating the neutron (n) channel can be written as

$$P_{\rm n}(E_i^*) = \frac{\Gamma_{\rm n}(E_i^*)}{\Gamma_{\rm tot}(E_i^*)}, \tag{7}$$

where, $\Gamma_{\rm tot} = \Gamma_{\rm n} + \Gamma_{\rm p} + \Gamma_\alpha + \Gamma_\gamma + \Gamma_{\rm f}$, which is addressed in detail in Ref. [38, 39]. The partial decay widths for the evaporation of neutron can be estimated by the Weisskopf-Ewing theory [40].

$$\Gamma_{\rm n}(E^*,J) = \frac{(2s_{\rm n}+1)m_{\rm n}}{\pi^2\hbar^2\rho(E^*,J)} \times \int_{I_{\rm n}} \varepsilon\rho(E^* - B_{\rm n} - \varepsilon, J)\sigma_{\rm inv}(\varepsilon)d\varepsilon. \tag{8}$$

Compared to the standard Bohr-Wheeler fission width [41], we assume that the quantal penetration and reflection of the barrier can be represented by the Hill-Wheeler approximation [42]. In contrast to the standard Bohr-Wheeler fission width, we employ the modified version in which the fission barrier is treated as excitation energy dependent[16]. The modified Bohr-Wheeler fission width is:

$$\Gamma_{\rm f}(E^*,J) = \frac{1}{2\pi\rho_{\rm f}(E^*,J)} \times \int_{I_{\rm f}} \frac{\rho_{\rm f}(E^* - B_{\rm f} - \varepsilon, J)d\varepsilon}{1 + \exp[-2\pi(E^* - B_{\rm f} - \varepsilon)/\hbar\omega]}. \tag{9}$$

Here $\hbar\omega$ = 1 MeV. The fission barrier height $B_{\rm f}(E^*)$ in $\Gamma_{\rm f}$ is given as [43]

$$B_{\rm f}(E^*) = -E_{\rm sh}^0 {\rm e}^{-E^*/E_{\rm d}}, \tag{10}$$

here $E_{\rm sh}^0$ is the shell correction energy which is taken

from Ref. [44]. $E_{\rm d}$ is the damping factor of the shell effects.

III. RESULTS AND DISCUSSION

A. Fusion at the radial degree of freedom

The fusion barrier $B_{\rm fus}(J)$ is a key physical quantity for calculating the fusion probability. From the view point of radial degree of freedom (mostly related to quadrupole moment Q_{20}), the fusion could be considered as the reverse process of the fission with fixed octupole moment Q_{30}. $B_{\rm fus}(J)$ in Eq. (3) can be calculated as

$$B^{R}_{\rm fus}(J) = E_{\rm sd} - E_{\rm inj} + E^{\rm rot}_{\rm sd}(J) - E^{\rm rot}_{\rm inj}(J). \quad (11)$$

In this work, the deformation energies including the saddle point $E_{\rm sd}$ and the injection point $E_{\rm inj}$ are calculated by using the finite range liquid drop model (FRLDM) [63, 64]. The injection point $S_{\rm inj}$ denotes the closest touching configuration ($R_{\rm min}$) in capture process and an initial condition undergoing the shape evolution toward the compound nucleus by overcoming an inner barrier, expressed as $S_{\rm inj} = R_{\rm min} - (R_{\rm P} + R_{\rm T})$. Details of rotational energy $E^{\rm rot}_{\rm sd}(J)$ and $E^{\rm rot}_{\rm inj}(J)$ are given in Ref. [65].

As shown in Fig. 2(a), the fusion process is overcoming the inner fusion barrier with the evolution of the configurations from injection point to the saddle point. The position of injection point plays an important role in the fusion probability. The expression for the $S_{\rm inj}$ can be derived from the experimental data by fitting the calculations to the experimentally measured maximum values of the ERCS. The fitting results of the $S_{\rm inj}$ values as a function of the excess of the center-of-mass energy $E_{\rm c.m.}$ over the Coulomb barrier B_0 is shown in Fig. 2(b), where B_0 represents the nucleus-nucleus interaction potential in the entrance channel, which prevent the system from capture. The strong linear correlation between $S_{\rm inj}$ and $E_{\rm c.m.}$ - B_0 is shown and the systematics can be fitted as

$$S_{\rm inj} = 2.253\ {\rm fm} - 0.0165 \times (E_{\rm c.m.} - B_0)\ {\rm fm/MeV}. \quad (12)$$

It is evident from Fig. 2(b) that the injection distance $S_{\rm inj}$ increases as the value of $E_{\rm c.m.} - B_0$ decreases. This is because for the low incident energy the system has sufficient time for nucleon rearrangement, thereby facilitating neck formation at the relatively large distance. In contrast, for high incident energy, a more compressed configuration for neck formation is required. The same behavior is also shown in Ref. [67]. The strong correlation observed between the $S_{\rm inj}$ values and the corresponding energies $E_{\rm c.m.} - B_0$ provides support for the fission barriers proposed by Kowal et al [68].

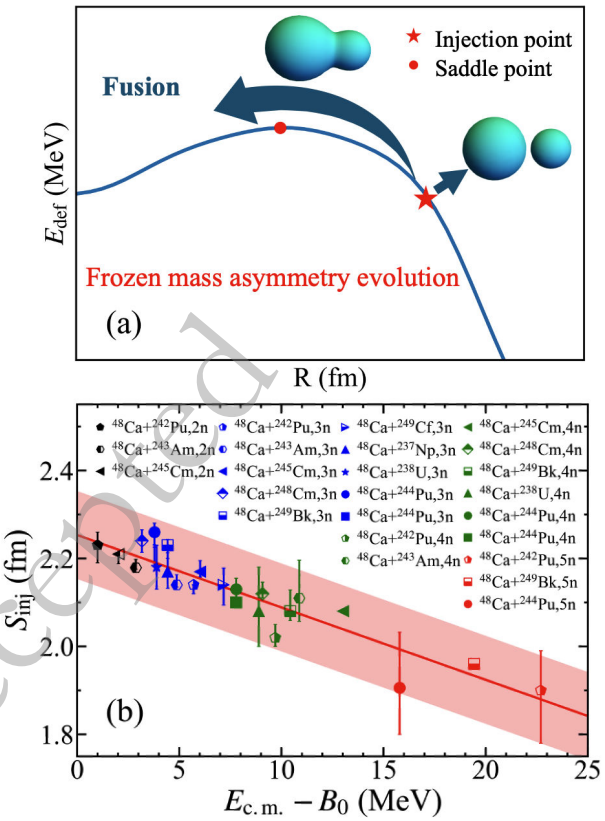

Fig. 2. (Color online) (a) Schematic depiction of the the fusion process in the radial degree of freedom. Red pentagram and red circle represent injection point and saddle point, respectively. (b) Systematics of the $S_{\rm inj}$ for the hot fusion reactions with ^{48}Ca projectiles as a function of $E_{\rm c.m.} - B_0$, deduced from analysis of experimental data [7, 10, 45−62]. The red shaded area in the figure represents the overall error of all $S_{\rm inj}$, which is obtained through weighted least squares fitting. The error bars for each $S_{\rm inj}$ are derived from the upper and lower limits of the error bars of the experimental values.

Eq. (12) determines the systematics of the injection point. Fig. 3 shows the comparison of the calculated ERCS by using the Eq. (12) with the experimental data. The calculated ERCS (solid lines) can reproduce the experimental data within the error bar rather well. Therefore, the systematical behavior for $S_{\rm inj}$ as well as the good description of the experimental data show that the Smoluchowski diffusion equation at the radial degree of freedom is a reasonable approach for investigating the extrapolation behavior to heavier projectiles.

B. Fusion at the mass asymmetry degree of freedom

Fission is a slow process dominated by neck evolution dynamics. Similarly, the fusion process has sufficient time for shape relaxation. To strengthen the reliability of theoretical results, it is worth studying the fusion process from different perspectives: the mass asymmetry degree of freedom (mostly related to Q_{30}). In low-energy

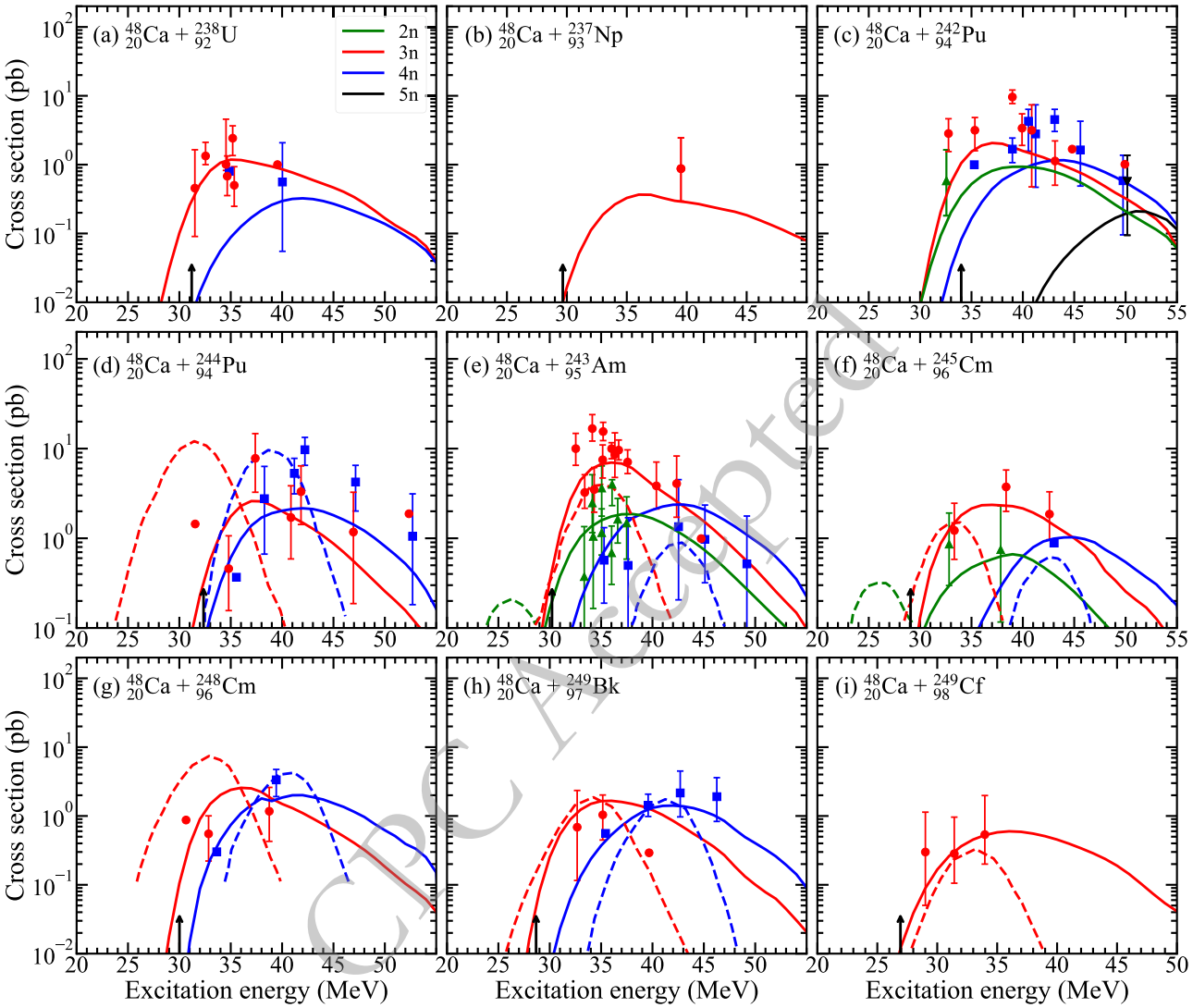

Fig. 3. (Color online) In terms of radial degree of freedom (solid lines), the calculated ERCS are compared with the available experimental data for the reactions ^{48}Ca+^{238}U [45] (a), ^{48}Ca+^{237}Np [10, 46] (b), ^{48}Ca+^{242}Pu [45, 47, 48] (c), ^{48}Ca+^{244}Pu [7, 49−51] (d), ^{48}Ca+^{243}Am [46, 52, 53] (e), ^{48}Ca+^{245}Cm [10, 49, 54] (f), ^{48}Ca+^{248}Cm [45, 55−57] (g), ^{48}Ca+^{249}Bk [10, 46, 58−62] (h), and ^{48}Ca+^{249}Cf [54, 60] (i). The calculated ERCS in the channels 2n, 3n, 4n, and 5n are denoted by the green lines, red lines, blue lines, and black lines, respectively. Here, dash lines denote the results from previous theoretical work [66]. Vertical arrows denote the excitation energies corresponding to collisions at $E_{\rm c.m.} = B_0$ for each reaction.

heavy-ion nuclear reactions, nucleon transfer and mass rearrangement between colliding partners play a crucial role.

In view of these physical features, the mass asymmetry is usually selected as a key macroscopic variable to describe fusion process. We also obtain an approximately inverted parabolic potential energy surface and investigate the fusion based on the Smoluchowski diffusion equation. In the nuclear fusion process under the mass-asymmetry degree of freedom, the evolution in radial is frozen and the nucleon transfer takes place at the contact position which can be described by the distance between surfaces of the two colliding nuclei ($D_{\rm cont}$). The reaction of the system towards fusion generally refers to the transfer of nucleons from the lighter nucleus (either the projectile or the target) to the heavier nucleus, evolving in the direction of increasing the mass asymmetry η. The evolution of this process can be described by the diffusion of the mass asymmetry degree of freedom η (see Fig. 4(a)) [69].

Following the capture of the projectile by the target nucleus after overcoming the Coulomb barrier, forming a composite system, fusion takes place and the compound nucleus is formed when the dinuclear system overcomes the inner fusion barrier $B_{\rm fus}$. The more asymmetry configurations than those on the B.G. point are considered as the occurrence of fusion [38]. $B_{\rm fus}$ is calculated to be equal to the difference between the driving potential at

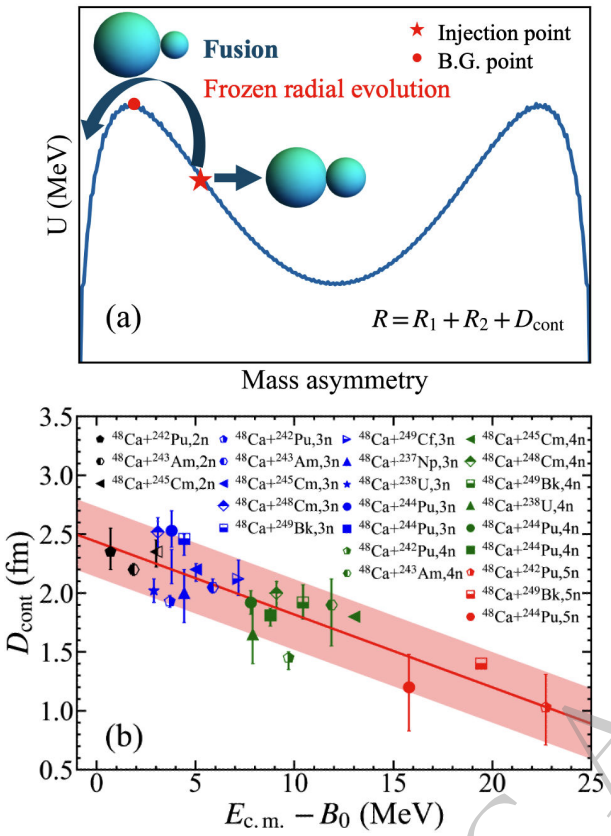

Fig. 4. (Color online) (a) Schematic depiction of the fusion process in mass asymmetry degree of freedom. Red pentagram and red circle represent injection point and B.G. point, respectively. (b) The same way as in Fig. 2(b), dependence of the $D_{\rm cont}$ on $E_{\rm c.m.}-B_0$. The error bars are calculated in the same way as those in Fig. 2.

the B.G. point and the driving potential at the injection point (η of the projectile-target combination), as shown in Fig. 4(a). $B_{\rm fus}$ is mainly determined by the details of the potential energy surface (PES) which is the potential energy of the dinuclear system along the η direction and can be written as

$$\begin{aligned} &U(Z_1,N_1,R=R_1+R_2+D_{\rm cont})=\Delta(Z_1,N_1)\\ &+\Delta(Z_2,N_2)+V(Z_1,N_1,R=R_1+R_2+D_{\rm cont}), \end{aligned} \tag{13}$$

here, R_1 and R_2 are the radii of the two nuclei. $\Delta(Z_i,N_i)(i=1,2)$ is the mass excess of the ith fragment [70]. $V(Z_1,N_1,R=R_1+R_2+D_{\rm cont})$ is the nucleus-nucleus interaction potential. Here, $D_{\rm cont}$ refers to the surface distance between two colliding nuclei for nucleon transfer process taking place [38].

$B^{\eta}_{\rm fus}(J)$ can be calculated as

$$B^{\eta}_{\rm fus}(J)=U(\eta_{\rm B.G})-U(\eta_i). \tag{14}$$

Similarly, the relationship between the contact distance $D_{\rm cont}$ and $E_{\rm c.m.}-B_0$ is shown in Fig. 4(b), within the error bar a linear relationship between $D_{\rm cont}$ and $E_{\rm c.m.}-B_0$ is obtained. This interesting behavior represent that the consideration of the Smoluchowski diffusion equation at the mass asymmetry degree of freedom is reasonable. The systematical behavior can be written as

$$D_{\rm cont}=2.435\ {\rm fm}-0.0618\times(E_{\rm c.m.}-B_0)\ {\rm fm/MeV}. \tag{15}$$

Unexpectedly, we observe that the inner fusion barrier exhibits a systematic similarity in the mass asymmetry and radial degrees of freedom. This suggests that to some extent the descriptions of the fusion process of both degrees of freedom share similarities and are comparable. Both perspectives are important reaction degrees of freedom in the fusion process. Studying the fusion reactions from multiple perspectives is crucial for verifying the reliability of the theoretical extrapolation from ^{48}Ca to ^{54}Cr.

In order to verify the method, by using Eq. (15) the calculated ERCS in ^{48}Ca induced reactions are compared with the experimental data, as shown in Fig. 5. The calculated results (dashed lines) are in good agreement with both the experimental ERCS and the optimal energies. The above results give us confidence based on the Smoluchowski diffusion equation at mass asymmetry degree of freedom to investigate the ERCS of fusion reactions leading to new elements. In Fig. 5, we also compare our results with those from the previous work Ref. [66]. It is found that the 3n evaporation channel is dominant, which is consistent with the results in Ref. [66]. We observe that for the reactions ^{48}Ca+^{243}Am and ^{48}Ca+^{245}Cm, our theoretical predictions agree better with experimental results than those reported in Ref. [66]. This is probably because in Ref. [66], the capture transmission coefficients T are calculated using a simple sharp cutoff approximation. This approach is known to underestimate the capture cross-section below the Coulomb barrier.

C. The extrapolation of projectiles with ^{50}Ti and ^{54}Cr

In the above calculations, we notice that the Smoluchowski diffusion equation based on the radial and mass asymmetry degrees of freedom describes the experimental data in ^{48}Ca induced reactions quite well. As we mentioned above, we need to clarify whether it is reasonable to extrapolate the model including the systematical behaviors of $S_{\rm inj}$ and $D_{\rm cont}$ in ^{50}Ti and ^{54}Cr induced reactions. Based on the values of $S_{\rm inj}$ and $D_{\rm cont}$ determined by Eq. (12) and Eq. (15). The calculated results in the reactions ^{50}Ti+^{242}Pu, ^{50}Ti+^{244}Pu, and ^{54}Cr+^{238}U are shown in Fig. 6. The calculated results for all reactions are in good agreement with the experimental data for both perspectives of radial and mass asymmetry degrees of freedom. The radial and mass asymmetric degrees of free-

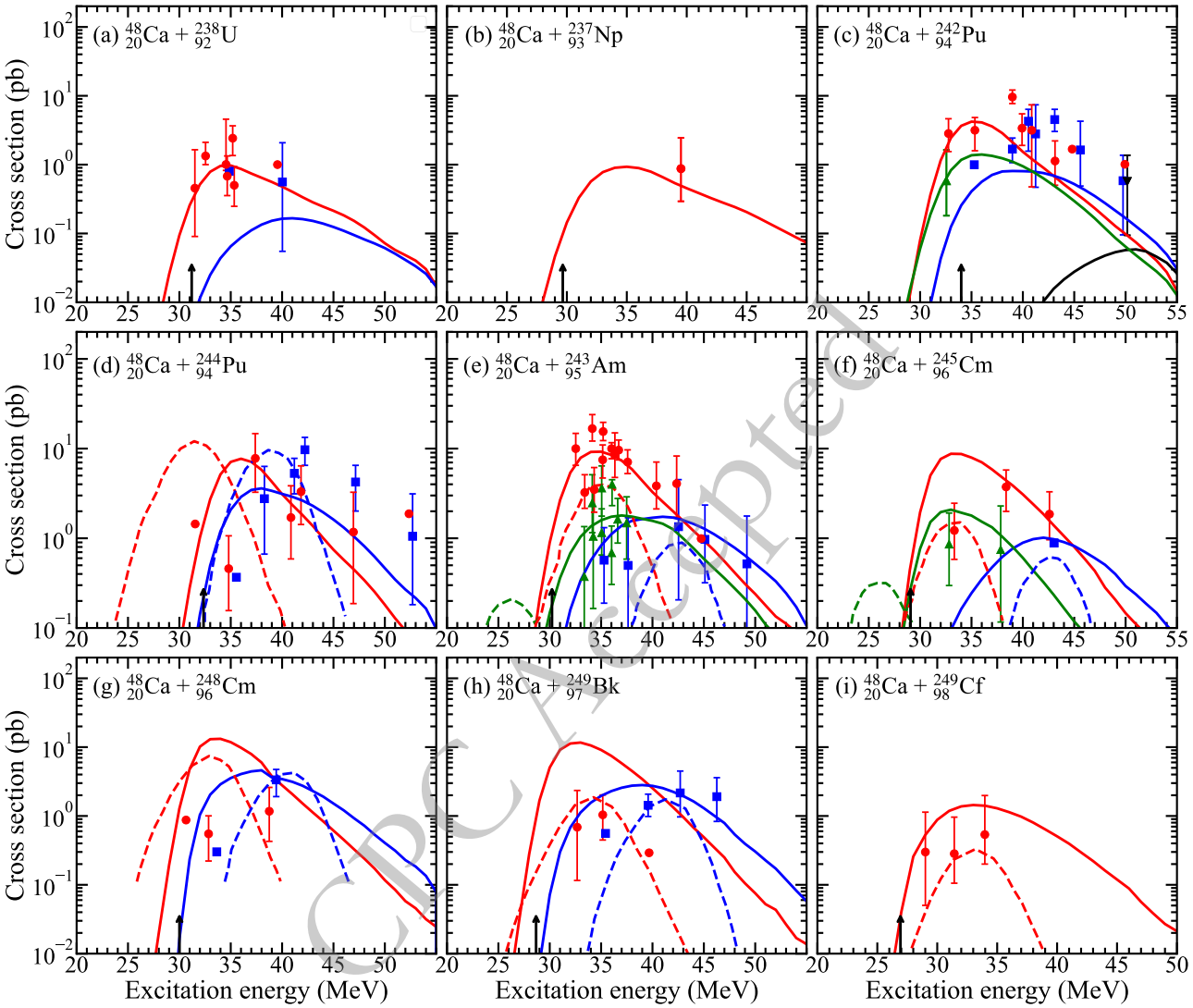

Fig. 5. (Color online) In terms of mass asymmetry degree of freedom (solid lines), the calculated ERCS are compared with the available experimental data for the reactions ^{48}Ca+^{238}U [45] (a), ^{48}Ca+^{237}Np [10, 46] (b), ^{48}Ca+^{242}Pu [45, 47, 48] (c), ^{48}Ca+^{244}Pu [7, 49−51] (d), ^{48}Ca+^{243}Am [46, 52, 53] (e), ^{48}Ca+^{245}Cm [10, 49, 54] (f), ^{48}Ca+^{248}Cm [45, 55−57] (g), ^{48}Ca+^{249}Bk [10, 46, 58−62] (h), and ^{48}Ca+^{249}Cf [54, 60] (i). The calculated ERCS in the channels 2n, 3n, 4n, and 5n are denoted by the green lines, red lines, blue lines, and black lines, respectively. Here, dash lines denote the results from previous theoretical work [66]. Vertical arrows denote the excitation energies corresponding to collisions at $E_{\rm c.m.} = B_0$ for each reaction.

dom are key degrees of freedom in fusion processes. These two degrees of freedom are usually considered in some theoretical models separately. For example, in the DNS model, the radial degree of freedom is frozen and the fusion process takes place in the mass asymmetry degree of freedom. In the FBD model, the fusion probability is calculated using the barrier, and penetrating the barrier occurs in the radial degree of freedom. In this work, we independently study the fusion process from two perspectives: radial and mass asymmetric degrees of freedom. We find that the parameter $S_{\rm inj}$ under radial degrees of freedom and $D_{\rm cont}$ under mass asymmetric degrees of freedom have a strong linear correlation with $E_{\rm c.m.} - B_0$. From a quantitative point of view, we also give the error range of $S_{\rm inj}$ and $D_{\rm cont}$. The final calculated ERCS is in good agreement with the experimental data. In Fig. 6, the extrapolation calculation results are in good agreement with the experimental data within the error range. It can be seen that the reliability of this extrapolation is relatively high. Our investigation shows that studying fusion via either the radial degree of freedom or the mass asymmetry degree of freedom leads to remarkably similar and comparable outcomes. Consequently, both can be reliably employed to investigate complex fusion mechanisms. We would like to state that the transition from ^{48}Ca to heavier projectiles, such as ^{50}Ti and ^{54}Cr is reasonable and reliable according to current theories.

Calculations show that the ERCS for the heavier pro-

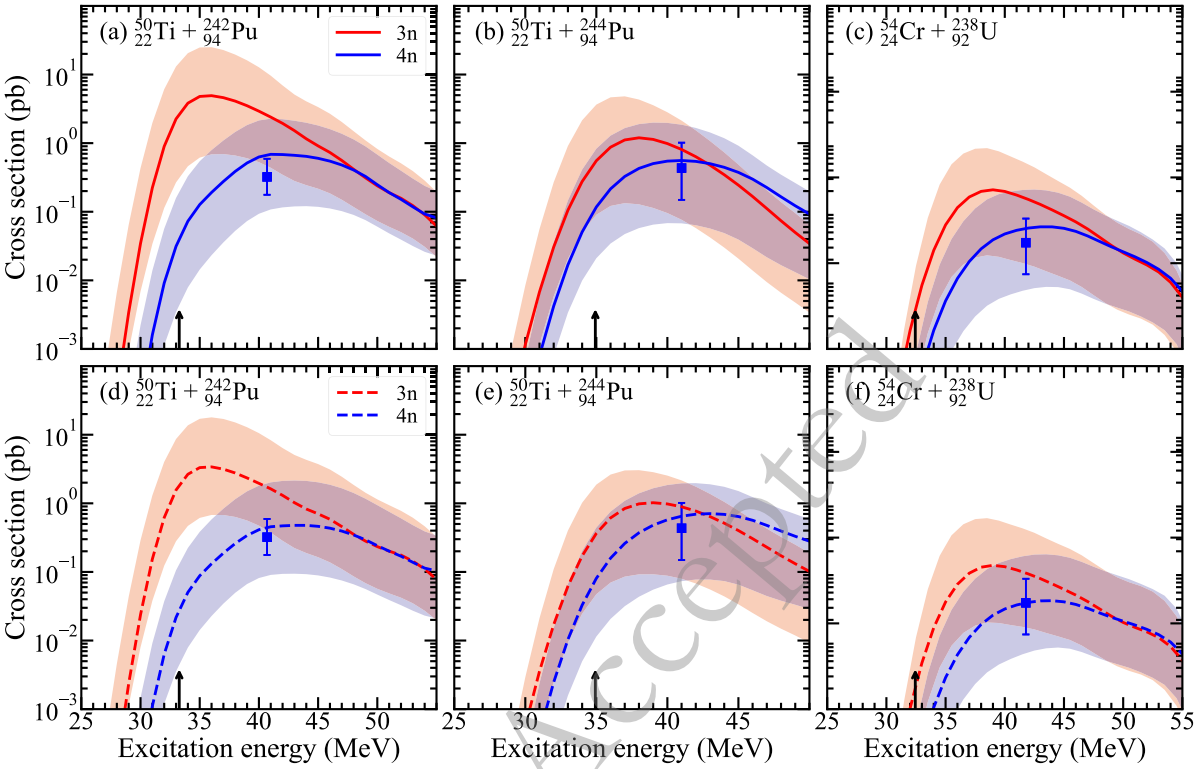

Fig. 6. (Color online) Comparison of the ERCS for reactions ^{50}Ti + ^{242}Pu, ^{50}Ti + ^{244}Pu, and ^{54}Cr + ^{238}U in radial degree of freedom (solid lines) and mass asymmetry degree of freedom (dashed lines) together with corresponding error corridors. Blue full squares represent experimental data for the 4n reaction channel of the reactions ^{50}Ti + ^{242}Pu [13], ^{50}Ti + ^{244}Pu [5], and ^{54}Cr + ^{238}U [13].

jectiles ^{50}Ti and ^{54}Cr in the synthesis of SHEs with $Z = 116$ are nearly one order of magnitude lower than that for the reaction induced by the ^{48}Ca projectile. This reduction is primarily due to the lower mass asymmetry in the entrance channel of the reactions involving ^{50}Ti and ^{54}Cr as projectiles, coupled with a higher fusion barrier. As a result, the system has a lower probability of fusion through diffusion.

To further investigate ERCS of synthesizing SHE with Z = 119. In Fig. 7, we conducted a study on the possibility of synthesizing superheavy nuclei $Z = 119$ using ^{50}Ti, ^{51}V, and ^{54}Cr as the projectiles. In the radial degree of freedom, the OIEs for producing the element with Z = 119 via the reactions ^{50}Ti + ^{249}Bk, ^{51}V + ^{248}Cm, and ^{54}Cr + ^{243}Am are estimated to be 224.5 MeV, 231.3 MeV, and 242.3 MeV, respectively. Correspondingly, under the mass asymmetric degree of freedom, the OIEs are predicted to be 224.5 MeV, 231.3 MeV, and 240.3 MeV, respectively. The predicted OIEs are close to the results from the OIE law proposed in Ref [11], especially for the reactions ^{50}Ti + ^{249}Bk and ^{54}Cr + ^{243}Am.

IV. SUMMARY

The ERCS for synthesizing SHEs based on the different perspectives (radial and mass asymmetry degrees of freedom) within the concept of Smoluchowski diffusion equation are investigated. By calibrating the injection point distance $S_{\rm inj}$ and contact distance $D_{\rm cont}$ as adjustable parameters using the experimental ERCS data from ^{48}Ca induced fusion reactions, we observe the strong linear systematic behaviors of $S_{\rm inj}$ and $D_{\rm cont}$ on $E_{\rm c.m.} - B_0$. The inner fusion barrier shows a systematic similarity in both the radial and mass asymmetry degrees of freedom, which suggests that to some certain extent radial and mass asymmetry degrees of freedom are similar and comparable in their description of the fusion process. The parameterization of $S_{\rm inj}$ and $D_{\rm cont}$ are then used for extrapolation to calculate the ERCS in the reactions ^{50}Ti + ^{242}Pu, ^{50}Ti + ^{244}Pu, and ^{54}Cr + ^{238}U. The calculated results show good agreement with the recent experimental data from LBNL [5] and Dubna [13], which indicate that the theoretical calculations are relatively reliable in extrapolating the projectiles from ^{48}Ca to ^{50}Ti and ^{54}Cr for synthesizing SHEs beyond Og. Finally, we present predictions of ERCS and OIEs for the synthesis of SHN with $Z = 119$ from both radial and mass asymmetry degrees of freedom. The predicted OIEs in radial and mass asymmetry degrees of freedom are consistent with each other, as well as the results in Ref. [11].

This work also inspires us to utilize microscopic theories (such as density functional theories [34, 71, 72] for calculating multidimensional PES and address it within the framework of the Smoluchowski diffusion equation.

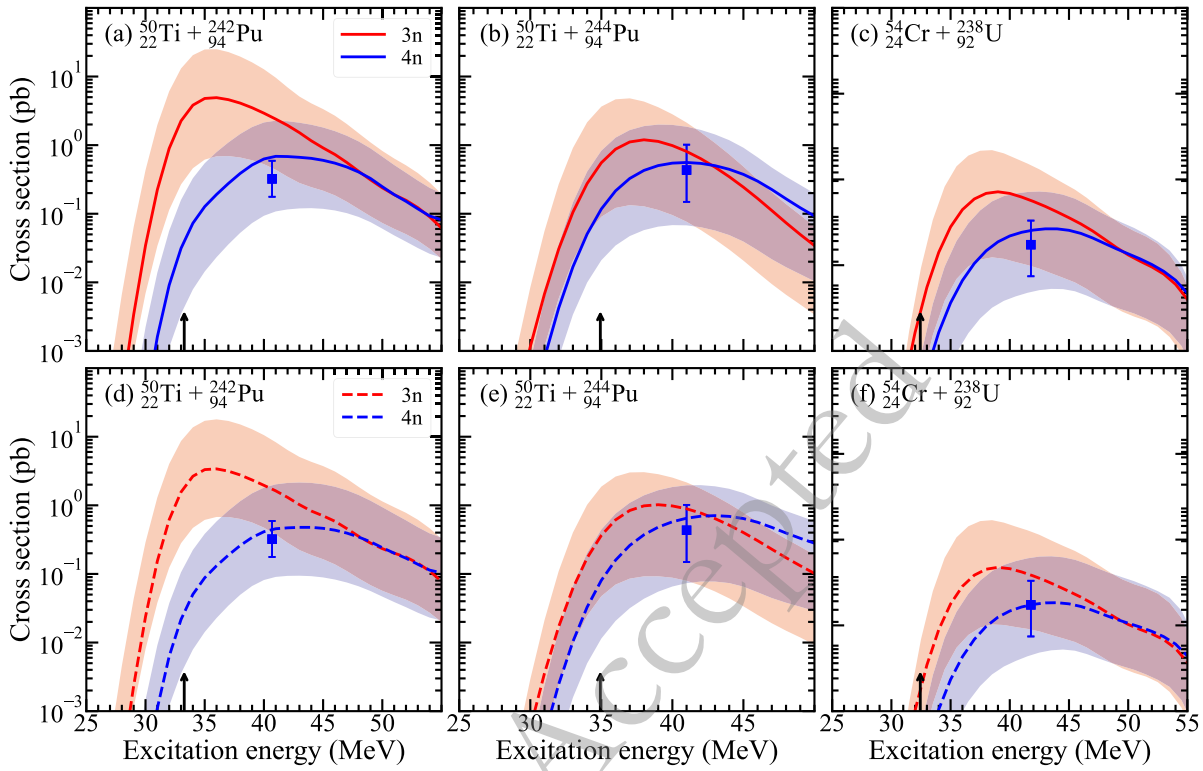

Fig. 7. (Color online) The ERCS production of new elements 119 through the reactions ^{50}Ti + ^{249}Bk, ^{51}V + ^{248}Cm, and ^{54}Cr + ^{243}Am predicted in radial degree of freedom (solid lines) and mass asymmetry degree of freedom (dashed lines) together with corresponding error corridors. The gray solid circles represent the maximum value of the ERCS for the 3n channels, corresponding to the optimal excitation energies.

References

[1] Yu. Ts. Oganessian, V. K. Utyonkov, Rep. Prog. Phys. **78**, 036301 (2015)
[2] W. Nazarewicz, Nat. Phys. **14**, 537 (2018)
[3] S. A. Giuliani, Z. Matheson, W. Nazarewicz, *et al.*, Rev. Mod. Phys. **91**, 011001 (2019)
[4] S. Hofmann, G. Münzenberg, Rev. Mod. Phys. **72**, 733 (2000)
[5] J. M. Gates, R. Orford, D. Rudolph, *et al.*, Phys. Rev. Lett. **133**, 172502 (2024)
[6] Yu. Ts. Oganessian *et al.*, Nature volume 400, pages242–245 (1999)
[7] Yu. Ts. Oganessian *et al.*, Phys. Rev. C **62**, 041604 (2000)
[8] Yu. Ts. Oganessian *et al.*, Phys. Rev. C **74**, 044602 (2006)
[9] Yu. Ts. Oganessian *et al.*, Phys. Rev. Lett. **104**, 142502 (2010)
[10] Yu. Ts. Oganessian *et al.*, Phys. Rev. C **87**, 014302 (2013)
[11] L. Zhu *et al.*, Phys. Rev. Res. **5**, L022030 (2023)
[12] K. Bourzac, Nature **632**, 16 (2024)
[13] Y. Oganessian, Eur. Phys. J. A **60**, 227 (2024)
[14] H. Lü, D. Boilley, Y. Abe, C. Shen, Phys. Rev. C **94**, 034616 (2016)
[15] X. J. Bao, Y. Gao, J. Q. Li, H. F. Zhang, Phys. Rev. C **91**, 064612 (2015)
[16] V. I. Zagrebaev, W. Greiner, Nucl. Phys. A **944**, 257 (2015)
[17] W. J. Swiatecki, K. Siwek-Wilczyńska, J. Wilczyński, Acta Phys. Pol. B **34**, 2049 (2003)
[18] Z.-H. Liu, J.-D. Bao, Phys. Rev. C **84**, 031602 (2011)
[19] J.-X. Li, F.-Y. Chen, H.-F. Zhang, Chin. Phys. C **50**, 034102 (2026)
[20] S. H. Zhu, T.-L. Zhao, X. J. Bao, Chin. Phys. C **48**, 124105 (2024)
[21] N. Wang, E.-G. Zhao, W. Scheid, S.-G. Zhou, Phys. Rev. C **85**, 041601 (2012)
[22] F. Li, L. Zhu, Z.-H. Wu *et al.*, Phys. Rev. C **98**, 014618 (2018)
[23] X.-B. Yu, L. Zhu, Z.-H. Wu, *et al.*, Nucl. Sci. Tech. **29**, 154 (2018)
[24] X. J. Bao, Phys. Rev. C **100**, 011601(R) (2019)
[25] J.-X. Li, H.-F. Zhang, Chin. Phys. C **47**, 124105 (2023)
[26] X.-Q. Deng, S.-G. Zhou, Phys. Rev. C **107**, 014616 (2023)
[27] P.-H. Chen, H. Wu, Z.-X. Yang, *et al.*, Nucl. Sci. Tech. **34**, 7 (2023)
[28] M.-H. Zhang, Y. Zou, M.-C. Wang, *et al.*, Nucl. Sci. Tech. **35**, 161 (2024)
[29] S.-H. Zhu, T.-L. Zhao, X.-J. Bao, Nucl. Sci. Tech. **35**, 124 (2024)
[30] R. S. Naik *et al.*, Phys. Rev. C **76**, 054604 (2007)
[31] Y. Fang, Z. Gao, Y. Zhang, *et al.*, Phys. Lett. B **858**, 139069 (2024)
[32] T. Cap, K. Siwek-Wilczyńska, J. Wilczyński, Phys. Rev. C **83**, 054602 (2011)

[33] K. Hagino, Phys. Rev. C **98**, 014607 (2018)
[34] X.-X. Sun, L. Guo, Phys. Rev. C **105**, 054610 (2022)
[35] W. D. Myers, W. J. Swiatecki, Nucl. Phys. A **601**, 141 (1996)
[36] Z. Gao, S. Liu, P. Wen, *et al*., Phys. Rev. C **109**, 024601 (2024)
[37] H. Risken, *The Fokker-Planck equation: methods of solution and applications*, pages 63–95. Springer (1989)
[38] L. Zhu, J. Su, Phys. Rev. C **104**, 044606 (2021)
[39] L. Zhu, J. Phys. G: Nucl. Part. Phys. **47**, 065107 (2020)
[40] V. F. Weisskopf, D. H. Ewing, Phys. Rev. **57**, 472 (1940)
[41] N. Bohr, J. A. Wheeler, Phys. Rev. **56**, 426 (1939)
[42] D. L. Hill, J. A. Wheeler, Usp. Fiz. Nauk **52**, 83 (1954)
[43] V. Yu. Denisov, I. Yu. Sedykh, Phys. Rev. C **98**, 024601 (2018)
[44] P. Möller, A. J. Sierk, T. Ichikawa, H. Sagawa, At. Data Nucl. Data Tables **109**, 1 (2016)
[45] Yu. Ts. Oganessian *et al*., Phys. Rev. C **70**, 064609 (2004)
[46] Yu. Ts. Oganessian *et al*., Phys. Rev. Lett. **108**, 022502 (2012)
[47] L. Stavsetra *et al*., Phys. Rev. Lett. **103**, 132502 (2009)
[48] P. A. Ellison *et al*., Phys. Rev. Lett. **105**, 182701 (2010)
[49] Yu. Ts. Oganessian *et al*., Phys. Rev. C **69**, 054607 (2004)
[50] Ch. E. Düllmann *et al*., Phys. Rev. Lett. **104**, 252701 (2010)
[51] J. M. Gates *et al*., Phys. Rev. C **83**, 054618 (2011)
[52] Yu. Ts. Oganessian, V. K. Utyonkoy, Yu. V. Lobanov, *et al*., Phys. Rev. C **69**, 021601 (2004)
[53] Yu. Ts. Oganessian *et al*., Phys. Rev. C **72**, 034611 (2005)
[54] Yu. Ts. Oganessian *et al*., Phys. Rev. C **74**, 044602 (2006)
[55] Yu. Ts. Oganessian *et al*., Phys. Rev. C **63**, 011301 (2000)
[56] Yu. Ts. Oganessian, V. K. Utyonkov, K. J. Moody, Phys. At. Nucl. **64**, 1349 (2001)
[57] S. Hofmann *et al*., Eur. Phys. J. A **48**, 1 (2012)
[58] Yu. Ts. Oganessian *et al*., Phys. Rev. Lett. **104**, 142502 (2010)
[59] Yu. Ts. Oganessian *et al*., Phys. Rev. C **83**, 054315 (2011)
[60] Yu. Ts. Oganessian *et al*., Phys. Rev. Lett. **109**, 162501 (2012)
[61] Yu. Ts. Oganessian *et al*., Phys. Rev. C **87**, 054621 (2013)
[62] J. Khuyagbaatar *et al*., Phys. Rev. Lett. **112**, 172501 (2014)
[63] A. J. Sierk, Phys. Rev. C **33**, 2039 (1986)
[64] Y. G. Huang, F. C. Gu, Y. J. Feng, *et al*., Phys. Rev. C **109**, 034609 (2024)
[65] P. N. Nadtochy, E. G. Ryabov, A. V. Karpov, D. V. Vanin, G. D. Adeev, Comput. Phys. Commun. **258**, 107605 (2021)
[66] K. Siwek-Wilczyńska, T. Cap, M. Kowal, *et al*., Phys. Rev. C **86**, 014611 (2012)
[67] K. Washiyama, D. Lacroix, Phys. Rev. C **78**, 024610 (2008)
[68] M. Kowal, P. Jachimowicz, A. Sobiczewski, Phys. Rev. C **82**, 014303 (2010)
[69] F.-S. Zhang, C. Li, L. Zhu, P. Wen, Front. Phys. **13**, 132113 (2018)
[70] L. Zhu, P.-W. Wen, C.-J. Lin, X.-J. Bao, J. Su, C. Li, C.-C. Guo, Phys. Rev. C **97**, 044614 (2018)
[71] M. Bender, K. Rutz, P.-G. Reinhard, *et al*., Phys. Rev. C **58**, 2126 (1998)
[72] K. Sekizawa, K. Hagino, Phys. Rev. C **99**, 051602 (2019)
[73] G. G. Adamian, N. V. Antonenko, W. Scheid, Phys. Rev. C **69**, 014607 (2004)